Science of the Total Environment 482–483 (2014) 325–335

Contents lists available at ScienceDirect

Science of the Total Environment

journal homepage: www.elsevier.com/locate/scitotenv

The impacts of a linear wastewater reservoir on groundwater recharge and geochemical evolution in a semi-arid area of the Lake Baiyangdian watershed, North China Plain

Shiqin Wang [a], Changyuan Tang [a,*], Xianfang Song [b], Qinxue Wang [c], Yinghua Zhang [b], Ruiqiang Yuan [d]

[a] Faculty of Horticulture, Chiba University, Matsudo-City 271-8510, Japan
[b] Key Laboratory of Water Cycle and Related Land Surface Processes, Institute of Geographic Sciences and Natural Resources Research, Chinese Academy of Sciences, Beijing 100101, China
[c] National Institute for Environmental Studies, Tsukuba 305-8506, Japan
[d] College of Environment and Resources, Shanxi University, China

HIGHLIGHTS

- An unlined wastewater reservoir caused the deterioration of groundwater quality.
- An evaporation fraction was estimated by Rayleigh distillation theory of isotopes.
- 73.5% of wastewater recharge to groundwater by leakage and irrigation infiltration.
- The region influenced by wastewater was divided into four subzones.
- Mixing, ion exchange, and carbonate precipitation are major geochemical processes.

ARTICLE INFO

Article history:
Received 2 July 2013
Received in revised form 22 February 2014
Accepted 22 February 2014
Available online 21 March 2014

Keywords:
Industrial wastewater reservoir
Groundwater recharge
Contamination
Geochemical processes
Lake Baiyangdian watershed

ABSTRACT

Sewage leakage has become an important source of groundwater recharge in urban areas. Large linear wastewater ponds that lack anti-seepage measures can act as river channels that cause the deterioration of groundwater quality. This study investigated the groundwater recharge by leakage of the Tanghe Wastewater Reservoir, which is the largest industrial wastewater channel on the North China Plain. Additionally, water quality evolution was investigated using a combination of multivariate statistical methods, multi-tracers and geochemical methods. Stable isotopes of hydrogen and oxygen indicated high levels of wastewater evaporation. Based on the assumption that the wastewater was under an open system and fully mixed, an evaporation model was established to estimate the evaporation of the wastewater based on isotope enrichments of the Rayleigh distillation theory using the average isotope values for dry and rainy seasons. Using an average evaporation loss of 26.5% for the input wastewater, the estimated recharge fraction of wastewater leakage and irrigation was 73.5% of the total input of wastewater. The lateral regional groundwater inflow was considered to be another recharge source. Combing the two end-members mix model and cluster analysis revealed that the mixture percentage of the wastewater decreased from the Highly Affected Zone (76%) to the Transition Zone (5%). Ion exchange and redox reaction were the dominant geochemical processes when wastewater entered the aquifer. Carbonate precipitation was also a major process affecting evolution of groundwater quality along groundwater flow paths.

1. Introduction

With industrialization and accelerated urbanization, municipal sewage leakage has become an important source of groundwater recharge, resulting in adverse effects on groundwater quality (McArthur et al., 2012; Schirmer et al., 2013). This is especially true for aquifers located in arid/semi-arid climate regions in which global warming and anthropogenic activities have led to decreased runoff, drying of rivers and declining groundwater levels. The major non-agricultural sources of groundwater contamination include leakage from water supply and disposal networks such as evaporation ponds, on-site sewage disposal, and contaminated land and rivers (Wakida and Lerner, 2005). Among these sources, evaporation ponds have been widely used in arid regions for the storage and disposal of wastewater (Geophysics Study Committee, 1984; Al-Kharabsheh, 1999). Although these ponds are often lined, many are unlined and therefore have the potential to impact groundwater quality via leakage. To effectively manage water resources within a basin, it is important to investigate the impacts of polluted

* Corresponding author. Tel.: +81 47 308 8911 (office).
E-mail address: cytang@faculty.chiba-u.jp (C. Tang).

http://dx.doi.org/10.1016/j.scitotenv.2014.02.130
0048-9697/

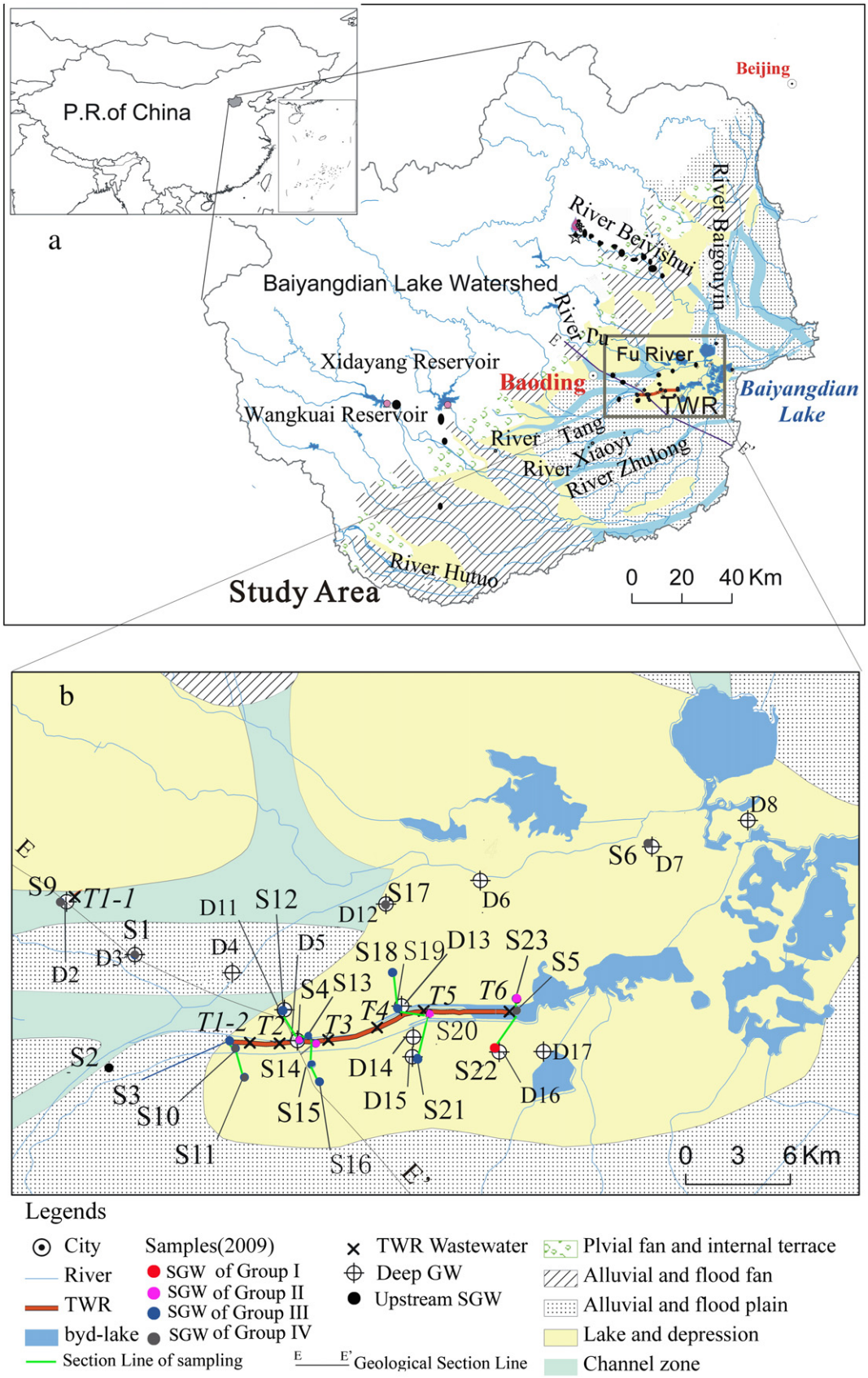

Fig. 1. Location of the study area in Lake Baiyangdian watershed (a) and sampling points in the study area (b).

rivers and surface wastewater systems on groundwater recharge and to recognize the geochemical evolution in groundwater.

Groundwater contamination is a major water problem in the Lake Baiyangdian watershed near Beijing, China (Fig. 1(a)). In this region, rivers are typically polluted, which has greatly threatened the quality of groundwater resources. Among the eight rivers that flow into Lake Baiyangdian, the only one that has perennial flow is the Fu River, which is mainly sourced by municipal sewage with or without primary treatment from Baoding (Qiu et al., 2009). The Tanghe Wastewater Reservoir (TWR) is a large linear wastewater reservoir located 20 km east of Baoding in the Lake Baiyangdian watershed. The TWR was constructed parallel to the Tang River to store industrial effluent from Baoding in 1975. A sluice gate was set in the east end of the channel to prevent the effluent from flowing into Lake Baiyangdian. Industrial wastewater drained to this reservoir is not treated, which leads to concentrations of water soluble chemicals that are much higher than those in other sewage and has resulted in the TWR becoming a linear source of regional groundwater contamination. Therefore, there is an urgent need to investigate the impacts of the wastewater reservoir on groundwater.

To study the impacts of polluted surface water on groundwater contamination, increasing attention has been paid to the interactions of groundwater–surface water (Petelet-Giraud et al., 2007; Kumar et al., 2009; Guggenmos et al., 2011; Al-Charideh and Hasan, 2012). Indirect methods, based on water balancing and solute balancing, are suitable methods for larger scale assessments but suffer from a significant uncertainty (Rieckermann et al., 2005; Chisala and Lerner, 2008). Direct methods such as tracer tests are less uncertain and have been applied to investigate the groundwater recharge sources and determine the migration pathways of the pollutant (Rieckermann et al., 2005). The most widely applied tracers include heater, environmental isotopes, and solute concentrations. In recent years, the multivariate statistical methods combined with geochemical processes of major ions have been testified as the effective approaches to interpret the present water chemicals characteristics and evolution (Belkhiri et al., 2010). Uncertainties in each approach to estimating recharge underscore the need for application of multiple techniques to increase reliability of recharge estimates (Scanlon et al., 2002).

This study investigated the TWR and the groundwater surrounding it in the Lake Baiyangdian watershed, China using multiple techniques. The specific goals of this paper were to: (1) evaluate the influences of the TWR on groundwater (i.e., extent and range), (2) estimate the quantity and percentage of groundwater recharge from the TWR and (3) elucidate the hydrogeochemical evolution along the water flow path.

2. Site description and hydrogeological characterization

The study area is located in the plains area of the Lake Baiyangdian watershed (Fig. 1(b)). The topographic features of the region include the lake and related depressions. The TWR is an unlined wastewater reservoir and with a length of 17.5 km and a width of 100 m, giving a maximum storage capacity of 8×10^6 m^3. An alluvial flood plain and ancient river channels are distributed in the south and west of the study area (Wu, 2008). The region is characterized by a temperate continental monsoon climate with an annual average rainfall of 510 mm (Cui et al., 2010) and evaporation of 1369 mm (Liu et al., 2006). The majority of precipitation (75%) falls from June to September, while the majority of evaporation (54%) occurs from May to August. The mean annual air temperature is 13.8 °C and the mean absolute humidity is 61% based on data obtained from the Baoding weather station of China meteorological data sharing service.

The main stratigraphy of the plain area is composed of unconsolidated sediments of Quaternary Q4. Silt clay and clay are widely distributed in the aquifer (Fig. 2), which can be divided into four groups according to its stratigraphic features (aquifer groups I, II, III and IV). Groups I and II include the Holocene Q_h, upper Pleistocene Q_p^3 and mid Pleistocene Q_p^2, while groups III and IV include the Lower Pleistocene Q_p^1 and the Tertiary Q_n stratigraphy, respectively. The shallow groundwater aquifer is composed of groups I and II, while the deep groundwater aquifer is composed of groups III and IV (Wang et al., 2008). Drilling data provided by China Geological Survey indicate that feldspar, mica and montmorillonite are major minerals in the aquifer.

3. Methods

3.1. Sampling and analytical procedures

A field survey and sampling were mainly conducted in June, 2009. Two wastewater samples were collected from the TWR in Sept., 2008. Water table, pH, electrical conductivity (EC) and temperature (T) were measured in situ using a portable meter (WM-22EP) (DKK, TOA Corporation, Japan). Groundwater is divided into shallow groundwater (SGW) with depth less than 100 or 120 m and deep groundwater (Deep GW) with depth greater than 100 or 120 m (Wang et al., 2013). Water samples were also collected from the shallow aquifer upstream of Baoding (Upstream SGW) and the deep aquifer (Deep GW). Samples of the study area included wastewater from the TWR (T1-2, T2–T6) and shallow groundwater (S1–S23) (Fig. 1(b)). The industrial wastewater of Baoding is concentrated in a channel southeast of the city, where sample T1-1 was collected. The wastewater is then transported from site T1-1 into the TWR via an underground channel. All water samples for analysis of major water chemicals and stable isotopes (δ^2H, δ^{18}O) were collected in air-tight 100 ml polyethylene vials and sealed with adhesive tape to reduce evaporation. Water samples for analysis of the concentrations of Fe, Mn, Al and Si were acidified to a pH of less than 2 using HCl.

Near sites S13 and S14, two soil profiles were drilled from the surface to a depth of 200 cm and soil samples were collected at 10 cm intervals. Water leached from these soil samples using the method described by Scanlon et al. (2006) were analyzed for water chemical parameters as described below.

All water samples were passed through 0.2 μm filters before analysis. Samples were analyzed for major ions (Na^+, K^+, Ca^{2+}, Mg^{2+}, Cl^-, SO_4^{2-} and NO_3^-) by ion chromatography (Shimadzu LC-10 AD, Japan). Freeze and Cherry (1979) recommend that 5% was a reasonable error limit of percentages of ion balance for accepting the analysis as valid. The concentrations of Fe, Mn, Al and Si were determined by ICP-MS. SiO_2 was calculated according to the measured Si concentration. Stable isotopes (δ^2H, δ^{18}O) were measured by Isotope Ratio Mass Spectrometry (Finnigan MAT-253) at the Institute of Geographic Sciences and Natural Resources Research, Chinese Academy of Sciences (CAS). The δ^2H and δ^{18}O values were expressed in the standard δ-notation as the per mil (‰) difference from standard-VSMOW (Vienna Standard Mean Ocean Water). The δ^2H and δ^{18}O measurements were reproducible to an accuracy of ± 0.2 and ± 1.0‰, respectively.

3.2. Cluster analysis

Hierarchical cluster analysis (HCA) is an efficient method of analyzing and displaying complex relationships among a considerably large number of samples. This technique has been used in a number of studies to distinguish water quality characteristics (Kumar et al., 2009; Belkhiri et al., 2010; Zhang et al., 2012). Cluster analysis can be run in Q-mode, in which clusters of samples are sought, or in R-mode, where clusters of variables are desired. In the present study, the Euclidean distance, which gives the similarity between two samples, was used to compare samples (Otto, 1998). When combined with Ward's linkage method (Ward, 1963), cluster classification was performed on a normalized data set to produce the most distinctive groups in which each member of the group is more similar to its fellow members than to any member outside the group. R-mode HCA was used to classify parameters with similar features for all samples in the study area. Q-mode HCA was used to classify the samples influenced by the TWR into different groups according to eleven water quality variables (pH, EC, Na^+, K^+, Ca^{2+}, Mg^{2+}, Cl^-, SO_4^{2-}, NO_3^-, HCO_3^- and SiO_2). The water chemical data of the samples was statistically analyzed using the STATISTICA (1998) software.

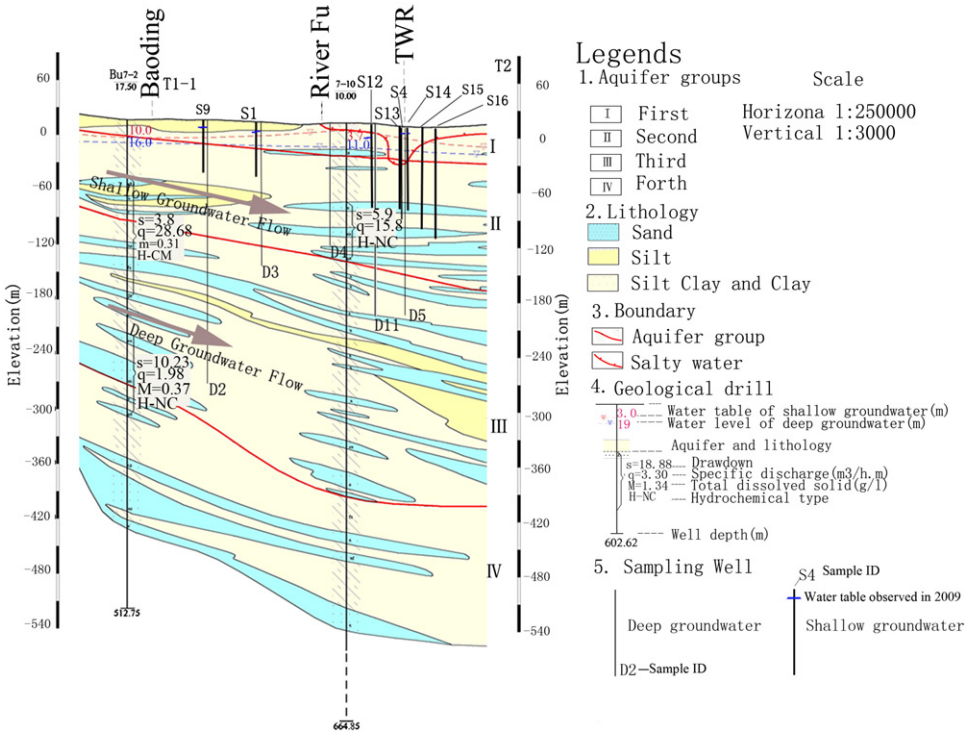

Fig. 2. Section profile and flow path along the profile of E–E′ in Fig. 1 (modified according to Zhang et al. (2009)).

3.3. Rayleigh evaporation model of stable isotopes

Craig and Gordon (1965) developed the Craig–Gordon (CG) model to describe the isotopic composition of an evaporative flux of water. There are several parameters that are needed to use this model, including 'the free-atmosphere' of the water body and the equilibrium and kinetic fractionation (Horita et al., 2008). A simple model of stable isotopes of hydrogen and oxygen can be developed incorporating both the equilibrium and kinetic enrichment factors of water that has undergone evaporation (Butler, 2007). The general form of a Rayleigh distillation equation states that the isotope ratio of the reactant in a diminishing reservoir is a function of its initial isotopic ratio (R_0), the remaining fraction of that reservoir (f) and the fractionation factor (ε, $\varepsilon = \alpha_{v-w} - 1$) for the reaction, which incorporates both equilibrium (ε_{w-v}) and kinetic fractionation ($\Delta\varepsilon_{v-bl}$) (Clark and Fritz, 1997).

$$R = R_0 f^{(\alpha_{v-w}-1)}. \tag{1}$$

After converting the isotope ratios to δ values, Eq. (1) can be given as:

$$\delta = \exp[\ln(f) \times (\varepsilon)/1000] \times (\delta_0 + 1000) - 1000. \tag{2}$$

The equilibrium isotope fractionation factor is strongly dependent on the temperature (T, in Kelvin degree) of the reaction, which can be determined at different temperatures through experimentation (Majoube, 1971; Horita and Wesolowski, 1994). In this study, the following equations were adopted to calculate the equilibrium fractionation factors of ^{18}O and ^{2}H between water and vapor (expressed as $10^3 \ln\alpha^{18}O_{v-w}$ and $10^3 \ln\alpha^{2}H_{v-w}$) (Majoube, 1971):

$$10^3 \ln\alpha^{18}O = 1.137\left(10^6/T^2\right) - 0.4156\left(10^3/T\right) - 2.0667 \tag{3}$$

$$10^3 \ln\alpha^{2}H = 24.844\left(10^6/T^2\right) - 76.248\left(10^3/T\right) + 52.612. \tag{4}$$

Kinetic effects are influenced by the surface temperature, wind speed, salinity and most importantly, humidity (Clark and Fritz, 1997). Gonfiantini (1986) described the kinetic effects in terms of humidity (h) using the following relationships:

$$\Delta\varepsilon^{18}O = 14.2(h-1) \tag{5}$$

$$\Delta\varepsilon^{2}H = 12.5(h-1) \tag{6}$$

where, $\Delta\varepsilon^{18}O_{v-bl}$ and $\Delta\varepsilon^{2}H_{v-bl}$ are kinetic fractionation factors of ^{18}O and ^{2}H between vapor and boundary layer in the evaporation interface.

3.4. Channel water balance

The channel water balance is described as (Lerner, 1997):

$$R = Q_{up} - Q_{down} + \sum Q_{in} - \sum Q_{out} - E_a - \frac{\Delta S}{\Delta t}, \tag{7}$$

where R is the recharge rate, Q is the flow rate, Q_{up} and Q_{down} are flows at the upstream and downstream ends of the reaches, Q_{in} and Q_{out} refer to tributary inflows and outflows along the reach, E_a is the evaporation from surface water or stream beds and ΔS is the change in storage in the channel and unsaturated-zone with time (Δt). The key issue for estimation of recharge is determination of the residual items. It should be noted that this approach is limited in that the accuracy of the recharge estimate depends on the accuracy of the residual items of a water balance. This limitation is critical when the magnitude of the recharge rate is small relative to that of the other variables, especially evaporation. However, averaging over longer time periods tends to reduce the impact of extreme precipitation events that are most responsible for recharge events (Scanlon et al., 2002).

As a case study of the TWR, it is assumed that the features of the channel bed are homogeneous. Q_{up} is the inflow rate (Q) of wastewater at the west end. Q_{out} is equal to zero because outflow is stopped by a sluice gate. It is also assumed that $\Delta S / \Delta t = 0$ because this study is not concerned with seasonal variation. Wastewater inflows, $\sum Q_{in}$, are equal to precipitation (P) because there is no inflow along the channel.

Since the TWR is an artificial reservoir with a river levee along two sides of a linear reservoir channel, the catchment for precipitation is limited to the water surface area. $\sum Q_{out}$ equals to the summation of evaporation (E) and irrigation water (I). Thus, the channel water budget of the TWR can be written as:

$$R + I = Q + P - E. \tag{8}$$

In this case, the summation of direct leakage and wastewater used by irrigation ($R + I$) was estimated, because it is difficult to investigate the quantity of irrigation water that is pumped directly from the TWR.

3.5. Mixing and geochemical models

Groundwater has many recharge sources. In this study, a simple material balance model was applied to partition the amount of water recharged into the shallow groundwater:

$$M_g C_g = \sum_{i=1}^{m} M_i C_i, \tag{9}$$

$$\sum_{i=1}^{m} M_i = 1, \tag{10}$$

where M and C represent the mass and concentrations of the solute per volume of each water body; g represents groundwater; $i = 1, 2, \ldots, m$, represent the different mixing sources.

Geochemical processes will modify the water chemical content along a flow path. The potential for a chemical reaction can be explained by the saturation index (SI) of a mineral, which reveals the chemical equilibrium of water with mineral phases. The SI of a mineral is calculated by:

$$\mathrm{SI} = \log(IAP/K), \tag{11}$$

where K is the equilibrium constant and IAP is the ion activity product. SI = 0 indicates equilibrium between the mineral and the solution; SI < 0 reflects subsaturation when dissolution is reached, and SI > 0 represents supersaturation, suggesting precipitation. The SI can be calculated by using the geochemical model of PHREEQC 2.15.0 (Parkhurst and Appelo, 1999).

4. Results and discussion

4.1. Water chemical characteristics

The means of field observations, major ions, heavy metals and isotopic components of water samples from different water bodies are listed in Table 1. An increasing trend in EC value and SO_4^{2-}, Ca^{2+}, Fe and Al ions was observed as follows: deep groundwater < upstream SGW < downstream SGW < TWR. The low concentrations of major ions (except Na^+) and smaller isotope components of deep groundwater verified the existence of an aquitard, which reduces the hydraulic connection between shallow and deep aquifers. Since it has been affected by polluted surface water, the water quality of the downstream SGW is worse than that of the upstream SGW and deep groundwater. Therefore, the means of the water chemical values of the upstream SGW and deep groundwater were referred to as the background value to investigate the impact of the TWR on the shallow groundwater downstream. The values based on field observations and major ions of the TWR and shallow groundwater in the study are listed in Table A.1 of Supplemental section. The changing patterns of concentrations of Si, Al, Mn and Fe were mainly used to discuss possible geochemical processes.

The results of HCA are illustrated in Fig. 3. The dendrogram of R-mode cluster analysis for all samples downstream divided the major variables into two main groups. The first group (group I) contains EC and SO_4^{2-} in close association. The electrical conductivity (EC) is positively correlated with the concentration of ions, the close association between EC and SO_4^{2-} suggests that the concentration of SO_4^{2-} has a large contribution to the total ion concentration. There are two subgroups in the second group (group II). Subgroup (1) comprises Na^+ and HCO_3^-. Since the major water chemical type of the wastewater in the TWR is Na–SO_4, the close similarity between Na^+ and HCO_3^- indicated that HCO_3^- is very closely associated with geochemical processes related to wastewater pollution. Subgroup (2) comprises other water chemicals such as Ca^{2+} and Mg^{2+} which have close similarity. The Q-mode cluster analysis classified water samples into four groups (Fig. 3(b)). (I) Sample S22 has the same linkage distance as sample T1-1, which indicates that it is a pollution source. The EC value and SO_4^{2-}, Na^+ and Cl^- concentrations at S22 are high. The field survey revealed that S22 were collected from area in which there were wells used to reject wastewater from a local factory. (II) Samples collected within 100 m of the TWR (S4, S20, S14), S23 and wastewater (T1-2 to T6) belong to the same group, which indicates these groundwater samples have a close connection to the TWR. Although S23 was located far from the TWR, it is believed that direct wastewater irrigation has influenced the water quality. The high occurrence of cancer in local residents of the village from which S23 was collected also suggests that there is poor water quality in this area. (III) Samples in this group can be further divided into two subgroups, one comprised of samples with medium connection to the wastewater (S3, S13, S15, S16 and S19), and another composed of samples with low connection to the wastewater (S12, S18 and S21). (IV) Samples in this group have little connection to the wastewater (S1, S5, S6, S9, S10, S11 and S17). Among these samples, only S10 and S11 are located on the south side of the TWR, which represents the edge of the TWR contamination. Other samples were collected from regions near the contaminated surface water or from the region irrigated by

Table 1
Means of field observation, major ions, heavy metals, and isotopes of different water bodies in Lake Baiyangdian Watershed.

Item	pH	T (°C)	EC (μS/cm)	Na^+ (mg/l)	K^+	Ca^{2+}	Mg^{2+}	Cl^-	NO_3^-	SO_4^{2-}	HCO_3^-	Si	Al	Mn	Fe	$\delta^2H/^1H$ (‰)	$\delta^{18}O/^{16}O$
TWR[a]	7.7	26.8	4553	836	22	202	47	232	71	2383	242	5.98	0.56	0.3	0.58	−41	−3.9
Downstream SGW[b]	8.2	15.9	2309	308	2.9	89	104	184	16	736	421	5.45	0.36	0.34	0.35	−60	−7.2
Upstream SGW[c]	8.0	15.5	710	21	5.5	83	30	30	41	70	285	7.22	0.22	0.15	0.16	−59	−7.5
Deep GW[d]	8.4	19.4	517	77	1.3	31	15	36	10	59	250	6.28	0.12	0.28	0.15	−74	−9.6
BYD[e]	8.5	28.3	1129	142	7.5	52	45	128	4	174	283	1.13	0.08	0.02	0.12	−26	−0.9

Note:
[a] Tanghe wastewater reservoir.
[b] Downstream shallow groundwater.
[c] Upstream shallow groundwater.
[d] Deep groundwater.
[e] Lake Baiyangdian.

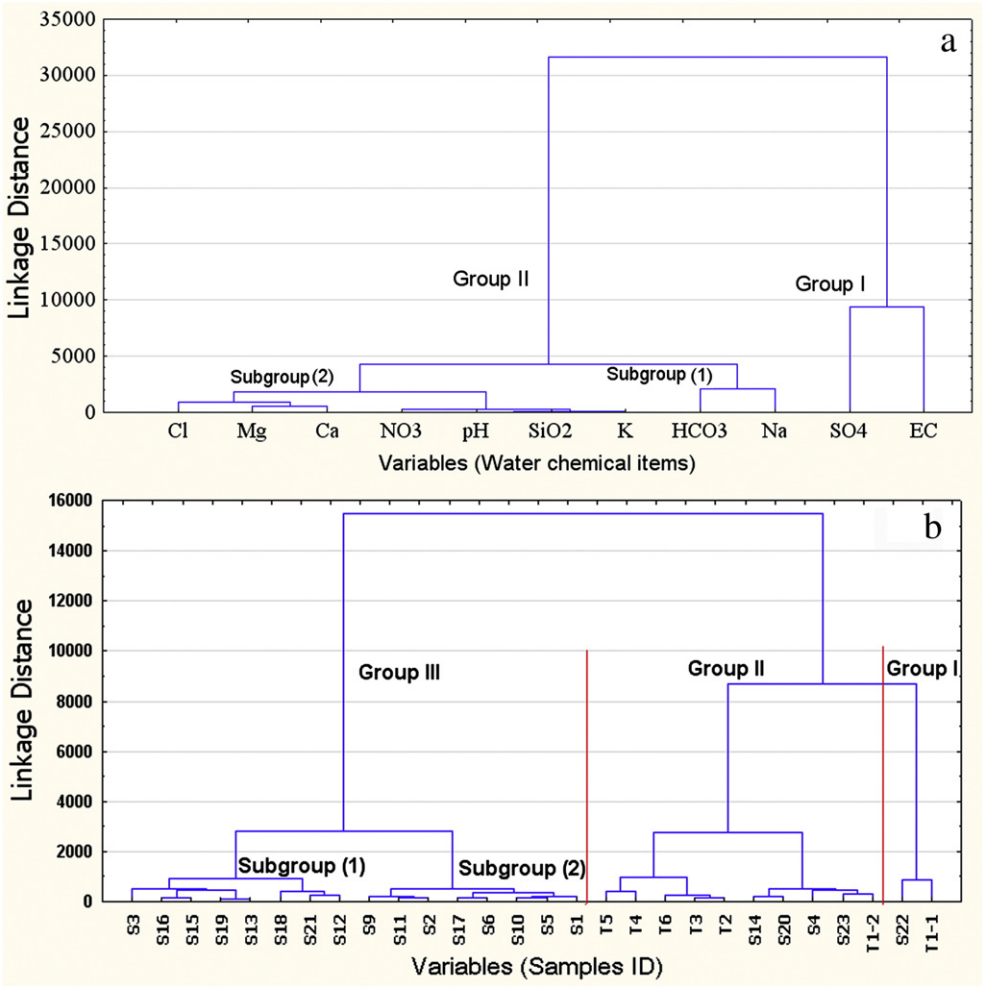

Fig. 3. Dendrograms showing R-mode HCA (a) and Q-mode HCA (b) for all samples in the study area.

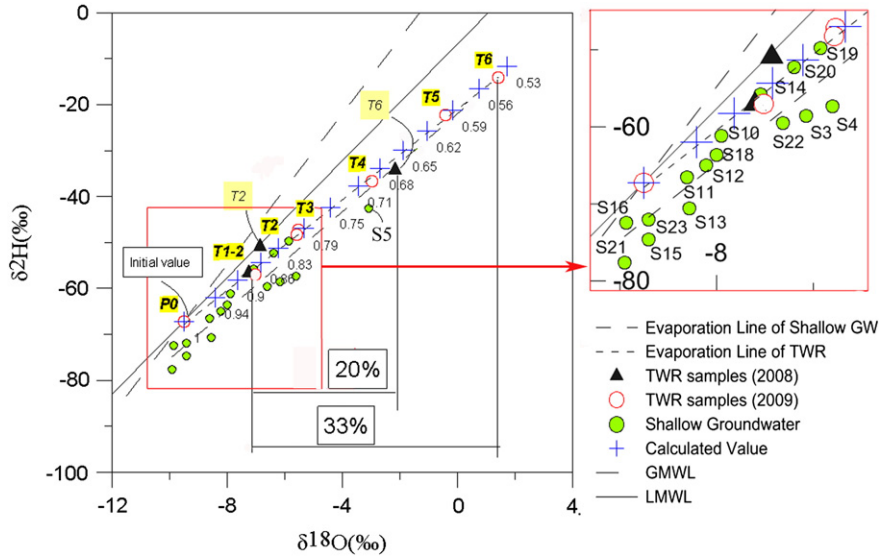

Fig. 4. Evaporation model of δ^2H and $\delta^{18}O$ of the TWR and shallow groundwater. The values of δ^2H and $\delta^{18}O$ were activities. The global meteoric water line (GMWL) is from (Craig, 1961). The local meteoric water line (LMWL) was obtained from the precipitation data of an experiment site in Lake Baiyangdian watershed. The evaporation line of the TWR is: $\delta^2H = 4.93 \times \delta^{18}O - 20.99$, $R^2 = 0.99$. The evaporation line of the groundwater is: $\delta^2H = 4.97 \times \delta^{18}O - 24.93$, $R^2 = 0.90$.

domestic sewage, where it is assumed that the TWR has no impact on groundwater quality. The remainder of this paper focuses on groundwater samples that were influenced by the TWR.

4.2. Evaporation and infiltration of the TWR

4.2.1. Evaporation model of the TWR based on Rayleigh distillation of isotopes

In this study, δ^2H and $\delta^{18}O$ values measured by combustion are reported as concentrations. Since only the free water molecules interact with the atmosphere, isotopic components in water with high salinity should be expressed as activities when modeling evaporation (Cartwright et al., 2009). Though the TDS of the TWR ranges from 3000 to 4500 mg/l, the differences between δ^2H activities and concentrations ranged from −0.10 to −0.12‰ and there was almost no difference between $\delta^{18}O$ activities and concentrations according to the calculation method of Horita (1989). Fig. 4 shows the relationship between δ^2H and $\delta^{18}O$ activities in wastewater of the TWR and nearby groundwater. The isotope components of samples collected during dry season (June, 2009) were larger than those collected in the rainy season (Sept., 2008). When water flowed along the river channel, the isotopes of the water that remained in the channel increased because of evaporation. The low slope ($s = 4.93$) of the evaporation line of the TWR suggests a semi-arid climate. The variation of isotopes from the initial point (T1-2) to the east point (T6) of the channel displays the isotopic features of Rayleigh distillation of an open system.

The average annual temperature of Baoding (13.8 °C) was plugged into Eqs. (3) and (4) to calculate the equilibrium fractionation factors. Correspondingly, the vapor–water isotope enrichment factors were −84.7 and −10.2‰ for δ^2H and $\delta^{18}O$, respectively. The evaporation line of the TWR extended backward to the intersect point (P_o) with GMWL and LMWL at −67 and −9.5‰ for δ^2H and $\delta^{18}O$, respectively (Fig. 4). The δ^2H values ranged from −100.2 to −2.39‰ and the $\delta^{18}O$ values varied from −12.6 to −0.15‰, respectively, at an experimental site upstream of the watershed during 2008 and 2009 (Yuan et al., 2011). Therefore, it is reasonable to consider the isotope values as the initial average values for wastewater of the TWR. The slope of the evaporation line of the TWR, 4.93, was used to find the best-fit line when using varying humidity values. The best-fit line was obtained when the humidity value was 50%, which is close to the average minimum humidity of 53% during the dry season. It should be noted that this model has several assumptions. Specifically, it is assumed that the reservoir is a steady state system with fixed inflow–outflow rates. Additionally, it is assumed that the water is fully mixed, and that all water is available for evaporative enrichment. To verify the assumption, two samples collected in surface and bottom of the middle part of TWR in 2011. Little difference of isotopes was found in water of different depth. The δ^2H of surface water and bottom water are −51.8 and −49.2‰, respectively. The $\delta^{18}O$ of surface water and bottom water are −5.93 and −5.67‰, respectively. Finally, Horita et al. (2008) pointed out that the environmental parameters of the C–G evaporation model constantly change over a short period of time. In this study, the evaporation during a year was based on the average values calculated in two time periods, the rainy season (September) and the dry season (June).

To understand the effects of the evaporation loss on wastewater in the TWR, the wastewater flowing into the TWR channel and aquifer was considered as one unit and the TWR was divided into six cells (Cell I to Cell VI). A conceptual model of evaporation and leakage can be described by parameters listed in Table 2, which shows the variation of isotopes and fraction of evaporation loss (f_e) and water remaining in the TWR and groundwater reservoir (f_r) in two seasons. When water flowed from the first cell to the second cell, a certain percentage of water was removed from the reservoir by evaporation, while additional water was lost via leakage and irrigation. Due to evaporation, isotope components have the linear increasing trends with the increasing distance along the channel ($\delta^2H = 0.50–7.4$, $R^2 = 0.963$; $\delta^{18}O = 2.5x–57.9$, $R^2 = 0.966$, where x is the distance from T1-2). This linear relationship indicates that the evaporation and leakage discharge is uniform. Evaporation also leads to an increase in the concentration of stable ions such as Na^+ and Cl^-. The results showed that there was a 26.5% evaporation loss from T1-2 to T6 in the dry season and 20% in the rainy season. Owing to the seasonal variation of the surface water, the mean evaporation loss (26.5%) of the dry and rainy season represents the annual evaporation loss of the TWR. Correspondingly, 73.5% of wastewater was recharged into groundwater by direct leakage and wastewater irrigation.

Influenced by the recharge from the TWR, the δ^2H and $\delta^{18}O$ in groundwater are distributed in the lower part of the LMWL (Fig. 4). Among these points, isotopes of site S5, which is located in the east of the TWR near Lake Baiyangdian, are larger than the other points. Water table loss from well abstraction in the study area not only has limited groundwater discharge into the lake, but has also accelerated lake leakage into the underlying aquifer systems (Moiwo et al., 2010). In addition, S5 contains Na–Mg–HCO_3–Cl type water, which is same as that of Lake Baiyangdian, but different from that (Na–Mg–SO_4–HCO_3) of groundwater influenced by the TWR. Taken together, these findings indicate that the water quality at S5 is more strongly influenced by Lake Baiyangdian than the TWR. The evaporation line of shallow groundwater has a similar slope (4.97) to that of the TWR (4.93), suggesting that evaporated wastewater has impacted the groundwater around the TWR.

4.2.2. Estimated evaporation based on the water balance of the river channel

The annual mean precipitation (510 mm, Cui et al., 2010) and evaporation (1369 mm, Liu et al., 2006) in the region of Lake Baiyangdian were used to calculate the items of Eq. (8). Therefore, the annual precipitation (P) input of TWR was calculated using the mean precipitation (P_a): $P = P_a \times A = 510 \times 10^{-3} \times 100 \times 17.5 \times 10^3 = 0.89 \times 10^6$ m^3/a. The evaporation of TWR was calculated as: $E = E_a \times A =$

Table 2
Estimated fractions of evaporation loss and wastewater remained in the TWR in dry and rainy season.

Cell number	ID	Dry season (June, 2009)							Rainy season (Sept., 2008)					
		f_r[a] (%)	f_e[b] (%)	Distance (km)	δ^2H (‰)	$\delta^{18}O$ (‰)	Na^+ (mg/l)	Cl^- (mg/l)	f_r[a] (%)	f_e[b] (%)	δ^2H (‰)	$\delta^{18}O$ (‰)	Na^+ (mg/l)	Cl^- (mg/l)
	P0	100	0		−67	−9.5			100	0				
I (P9 → T1-2)	T1-2	87	13	0	−57	−7.0	695	192	87	13	−58	−7.8		
II (T1-2 → T2)	T2	80	20	3	−47	−5.5	659	243	85.5	14.5	−51	−6.9	420	214
III (I2 → T3)	T3	79	21	6	−48	−5.6	725	241						
IV (T3 → T4)	T4	69.5	30.5	9	−37	−3.0	769	266						
V (T4 → T5)	T5	59.5	40.5	13	−22	−0.4	812	231						
VI (T5 → T6)[c]	T6	54	46	17.5	−14	1.4	810	253	67	33	−34	−2.2	626	261

[a] f_r — is the fraction of wastewater remained in the TWR.
[b] f_e — is the fraction of wastewater lost by evaporation.
[c] The fractions in cell VI delegate the average values of the whole TWR for dry and rainy season, respectively.

$1369 \times 10^{-3} \times 100 \times 17.5 \times 10^3 = 2.40 \times 10^6$ m^3/a, where A is the surface area of the TWR. A field survey revealed that the TWR primarily accepted effluent from a particular company that reportedly released 0.03×10^6 m^3/d of treated wastewater in 1995. Therefore, the annual mean input of Q was deduced, which left 10.95×10^6 m^3/a as the input of TWR. Thus, the percentage of evaporation loss of the total wastewater is 21.9%. Though a pan evaporation experiment with an area of 20 m^2 in an experimental site in Hengshui showed an annual evaporation of 1206 mm, which is close to the evaporation of this study area, the uncertainty exists when the pan evaporation is apply to natural water bodies (Lowe et al., 2009). The major limitation of the water balance calculation is that the accuracy of the recharge estimate depends on the accuracy with which the other components in the water budget equation are measured (Scanlon et al., 2002). Besides the evaporation, the input component was estimated by the effluent discharge in 1995. As groundwater is the major water supply in this region and it was reported that the groundwater development changed little from 1990s to 2005 (Bai and Ning, 2007), we assumed that the input component (effluent discharge) is unchanged after 1995 in this case. So the uncertainties should be considered in the leakage percentage estimated by the water balance method. Comparison of the results of the water balance and the isotope methods revealed a 4.6% difference. Of these two methods, the input component is unnecessary in the isotope method. Therefore, the evaporation loss based on the theory of isotope enrichment provides another method for estimation of the evaporation of water.

4.3. Impacts of the TWR on groundwater quality

4.3.1. Variation of major ions in the TWR

Generally, evaporation and dilution lead to an increase and decrease of solute concentration, respectively. If the evaporation process is dominant, assuming that no halite mineral is precipitated, the Na/Cl ratio would be unchanged (Jankowski and Acworth, 1997). Only the concentrations of Na^+ and Cl^- increased along the TWR (Table A.1). Specifically, the Na/Cl ratio varied around 5 and the SI of halite mineral was around −5.5 along the TWR, indicating that the evaporation process is dominant. Concentrations of HCO_3^- and NO_3^- tended to decrease along the river channel of the TWR. Denitrification might be the only effect resulting in the decreasing NO_3^- concentration because there is no dilution along the TWR. According to our unpublished organic matter data (e.g., nonylphenol and octylphenol), there is abundant organic material in the TWR. Nitrate reduction via organic matter oxidation is an important process in aquifers that is bacterially catalyzed and can be written as:

$$5/4CH_2O + NO_3^- \rightarrow 1/2N_2 + 5/4HCO_3^- + 1/4H^+ + 1/2H_2O, \quad (12)$$

where, CH_2O is used as a simplified representation of organic matter. However, additional processes that affect HCO_3 include carbonate precipitation induced by increasing H^+ and HCO_3^- during nitrate reduction. In addition, the increasing Ca^{2+} and Mg^{2+} concentrations caused by evaporation resulted in the calcite and dolomite and solution remaining nearly in equilibrium from T1-2 to T4 as indicated by SI values of calcite and dolomite of approximately 0 (−0.5 to 0.46 and −1.1 to 0.03, respectively). When water flows to point T5, the SI values become larger than 1.1, suggesting supersaturation and precipitation of calcite and dolomite. Precipitation removes some of the Ca^{2+} and Mg^{2+} from the wastewater, resulting in decreasing Ca^{2+}, Mg^{2+} and HCO_3^- concentrations from T5 to T6. A calcium core was found in some drilling data of the study area reported by the China Geological Survey, providing evidence of calcite or dolomite precipitation. This process can be described by the following reaction:

$$2Ca^{2+} + Mg^{2+} + 3HCO_3^- + 3OH^- \rightarrow CaCO_3 + CaMg(CO_3)_2 + 3H_2O. \quad (13)$$

4.3.2. Two-end members mix model

Since the regional groundwater flow direction is NW–SW toward Lake Baiyangdian, the lateral regional groundwater from upstream is another recharge source in addition to the TWR. The mixture of the different water sources is the dominant effect leading to changes in the components of the groundwater.

Although Cl^- is considered a conservative ion that can be used to demonstrate mixing processes (Panno et al., 2006), it was not applied in this study. This is because complex fertilizer (N/P/K/Cl) application in the farmland of the study area can disturb the mixing calculation. Additionally, the water type of the TWR is Na–SO_4 and the concentrations of Na^+ and SO_4^{2-} are about 4 and 10 times larger than that of Cl^-, respectively. Consequently, the error associated with mixing calculated based on the Cl^- concentration will be enlarged. In our previous study, the SO_4^{2-} mass balance was used to calculate the mixture percentage of wastewater in groundwater recharge by using Eqs. (4) and (5) (Wang et al., 2013). Combining the wastewater percentage of groundwater recharge with the groups identified by Q-mode analyses enables the study area to be divided into four regions (Table 3). (1) The Highly Affected Zone consisted of samples S4, S20 and S14 within group II, where the percentage of wastewater ranges from 61 to 76%. These samples were collected within 100 m of the TWR. Groundwater in this region is closely connected to the TWR; therefore, the water quality in this area is influenced by wastewater directly. (2) The Medium Affected Zone consisted of samples S3, S13, S15, S16 and S19 in one subgroup of group III, where the percentage of wastewater ranges from 29 to 45%. These samples were collected from a distance greater than 100 m but still close to the TWR (S3 and S19), or from areas in which the hydraulic conductance was high (S15 and S16). For example, S15 and S16 are located in the south of the TWR, where the river channel and alluvial sediments of the Tang River has a high permeability. (3) The Low Affected Zone consisted of samples of S18, S21 and S12 in another subgroup of group III, where the percentage of wastewater ranges from 9 to 30%. These samples were collected far from the TWR. (4) The Transition Zone consisted of samples S10 and S11, which were collected from an area in which the TWR has little impact on the groundwater quality (5%). The percentage of wastewater could be affected by point source pollution with a high level of SO_4^{2-}. For example, some pesticide bottles were found near well S20, which could lead to increased SO_4^{2-}.

4.3.3. Geochemical evolution along wastewater movement paths

The ion ratios may be used to indicate the possible geochemical reaction during the processes of wastewater leakage and recharge to groundwater. The plot of Na versus SO_4 shows that the points of groundwater (except for S22 and S23) are located around the mixing line between the TWR and upstream SGW, which shows that the groundwater was diluted along the flow path (Fig. 5(a)). However, some samples fell above or below the mixing line, indicating that other processes also affect the ion concentrations.

4.3.3.1. From TWR to the Highly Affected Zone. The soil and aquifers contain abundant materials capable of absorbing chemicals from water (Appelo and Postma, 1994). The aquifers of the study area are dominated by silt clay and clay (Fig. 2). When the Na-enriched wastewater enters the aquifer, ion exchange occurs in which Na^+ is adsorbed onto clay minerals while Ca^{2+} and Mg^{2+} are released to the liquid phase (Appelo and Postma, 1994) as follows:

$$4Na^+ + Ca\text{–}X_2 + Mg\text{–}X_2\text{–}4Na\text{–}X + Ca^{2+} + Mg^{2+} \quad (14)$$

where X is the clay mineral. The potential adsorption and desorption for the soil mineral can be demonstrated by the water leached from soils at two profiles near the TWR. The soil profile is featured by the high Na^+ concentration and the low Ca^{2+} and Mg^{2+} concentrations (Fig. 6). The plot of Na versus Mg (Fig. 5(b)) also provides evidence of the ion exchange between the TWR and groundwater of the Highly Affected Zone.

Table 3
Samples in different wastewater-affected zones based on percentage of wastewater contributions to groundwater (modified from Wang et al., 2013).

Influencing range	Highly Affected Zone			Medium Affected Zone					Low Affected Zone			Transition Zone	
ID	S4	S14	S20	S3	S15	S16	S13	S19	S18	S21	S12	S10	S11
Percentage (%)	76	64	61	45	41	43	32	29	30	20	9	5	5

First, the Mg^{2+} concentration increases as the Na^{+} concentration decreases. Additionally, the mean Na/Cl ratios decrease from 4.9 to 4.1 on the north side and 3.9 on the south side, while the mean Mg/Cl ratios increase from 0.3 to 1.7 on the north side and to 1.8 on the south side (Table A.1). Although ion exchange reaction causes Ca^{2+} to be released to the water, a plot of Na versus Ca revealed no obvious change in Ca^{2+} concentration (Fig. 5(c)) or Ca/Cl ratio, which is assumed to indicate the precipitation of calcite and dolomite. Calculation of the SI values of the major minerals in the shallow aquifer indicated that the groundwater is close to saturation or supersaturated with respect to all carbonate phases (calcite and dolomite), suggesting the precipitation of carbonate phases (Fig. 7). According to Eq. (13), the Ca/Mg mole ratio of the removed concentration should be 2:1 throughout the process of calcite and dolomite precipitation; therefore, the concentration of Ca^{2+} that remained in the aqueous phase is smaller than that of Mg^{2+}.

The wastewater contains a number of organic materials. The redox reaction shown in Eq. (12) is considered to be the dominant process responsible for the decreased NO_3^- concentration and the increased HCO_3^- concentration. This redox reaction was demonstrated in our previous research (Wang et al., 2013) based on the nitrate isotopes. The nitrate isotope ($\delta^{15}N$) increased from the TWR to groundwater, indicating denitrification. This reaction also caused the increasing HCO_3/Cl ratios from the TWR to the groundwater of the Highly Affected Zone (from 0.6 to 1.9 on the north side to 2.5 on the south side).

4.3.3.2. Along the groundwater flow path in the aquifer. Fig. 7(a) shows that all samples are under-saturated (SI < 0) with respect to minerals of anhydrite and gypsum. The SI variation of these minerals has a decreasing trend along the flow path in accordance with variations in the mixing percentage, indicating a small effect of evaporate minerals and a significant contribution of wastewater to the groundwater. The groundwater is close to saturation or is supersaturated with respect to all carbonate phases. Calcite, dolomite and chlorite have been found in the lake and depression sediments of the North China Plain (data provided by China Geological Survey). As the distance from the TWR increases, the carbonate precipitation plays a dominant role in the variation of major ions instead of ion exchange. Owing to the carbonate precipitation, some percentage of Ca^{2+}, Mg^{2+} and HCO_3^- is removed from the aqueous phase, which causes the concentrations to decrease along the flow path (Fig. 5(b) and (c)). In Fig. 5(d), points of the HCO_3/(Ca+Mg) ratio are distributed around the 1:1 line, which suggests the calcite and dolomite precipitation occurs as

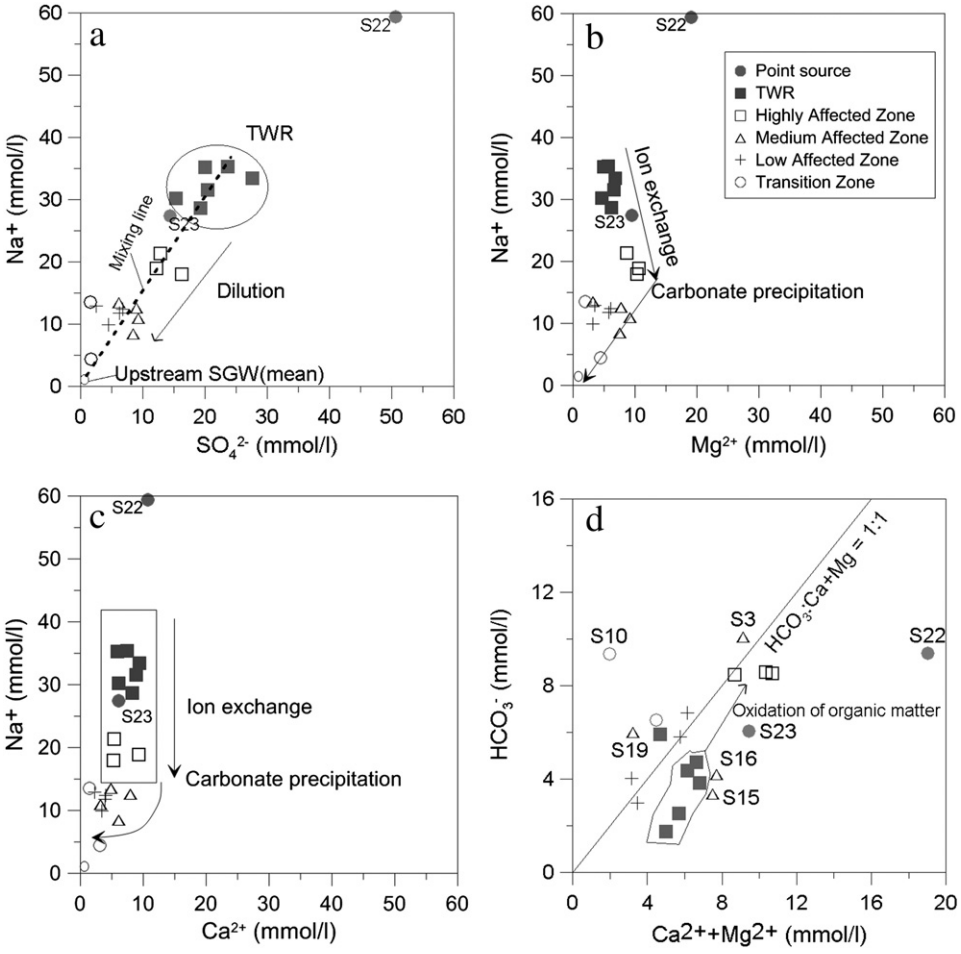

Fig. 5. Plots of Na/SO_4 (a), Na/Mg (b), Na/Ca (c) and $HCO_3/(Ca + Mg)$ showing ion variations caused by dilution, ion exchange, carbonate precipitation and silica weathering.

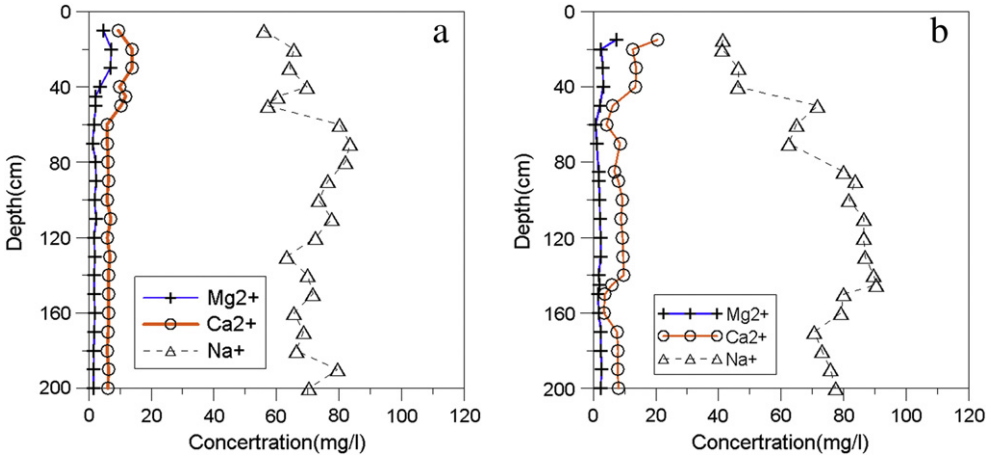

Fig. 6. Variations in ion concentrations in water leached from soil profile samples. (a) Soil profile of the area north of the TWR. (b) Soil profile of the area south of the TWR.

described by Eq. (13). Several exceptions (S11, S15 and S16) deviate from the 1:1 line in the plot of HCO_3 versus (Ca + Mg), indicating that these locations have been influenced by the content of organic matter in the local soil or aquifer.

5. Conclusions

The impacts of a man-made wastewater reservoir channel on the local shallow groundwater were revealed by comparing the characteristics of the wastewater reservoir channel to those of groundwater. When the cluster analysis was combined with the mixture percentage of wastewater identified in a previous study, the local groundwater could be further divided into a Highly Affected Zone, Medium Affected Zone, Low Affected Zone and Transition Zone, which had wastewater contributions ranging from 76 to 5%. The isotopic relationship of δ^2H and $\delta^{18}O$ suggested a strong evaporation effect for wastewater of the TWR and groundwater. Using the theory of the Rayleigh distillation based on the isotopic components of δ^2H and $\delta^{18}O$ activities, an average of 26.5% of water in the TWR was lost by evaporation. These findings indicate that an average of 73.5% of wastewater in the TWR was recharged into groundwater via leakage and irrigation infiltration. It should be noted that there are some limits to the accuracy of the estimation of isotopes. Specifically, the average annual evaporation was represented by the mean of the dry season and rainy season. Although this percentage is larger than the calculated channel water balance (21.9%), it provides an approach to estimate evaporation when the items of the water balance are unknown or large uncertainties exist in the residual items.

The ion ratios and calculated saturation of major minerals revealed that geochemical processes can change the water quality and the mixing effect. Ion exchange occurs in the TWR to the Highly Affected Zone via adsorption of Na onto clay minerals, while Ca and Mg are released to the groundwater. However, the carbonate precipitation removes much more Ca from the groundwater, which results in variations in the Ca concentration that is not obvious. A redox reaction led to a dramatic decrease of NO_3^- and increase of HCO_3^-. When water flows into an aquifer, carbonate precipitation becomes the dominant process to change the concentrations of major ions. However, it is difficult to quantify the extent to which different processes influence these variations because the depth of groundwater differs and does not follow the same flow path.

In summary, the results of this study showed that anthropogenic activities (urban lifestyles) have caused considerable damage to the groundwater quality downstream of the watershed. The natural evolution of groundwater chemicals has been considerably altered by input from the contaminated river and wastewater irrigation. In addition, sources of industrial pollution (TWR) have threatened groundwater quality to a greater extent. This study may help raise awareness regarding environmental impacts of wastewater reservoirs and stabilization ponds. Since groundwater is the major water supply for anthropogenic activities, especially in arid/semi-arid regions, measures should be taken to prevent linear pollution sources from impacting local groundwater. The results of the present study indicate that nitrate might not be a threat to groundwater owing to a redox reaction throughout the study area. Groundwater located within a distance of 100 m from the wastewater should be closely monitored because there is a direct hydraulic connection between this groundwater and the wastewater.

Supplementary data to this article can be found online at http://dx.doi.org/10.1016/j.scitotenv.2014.02.130.

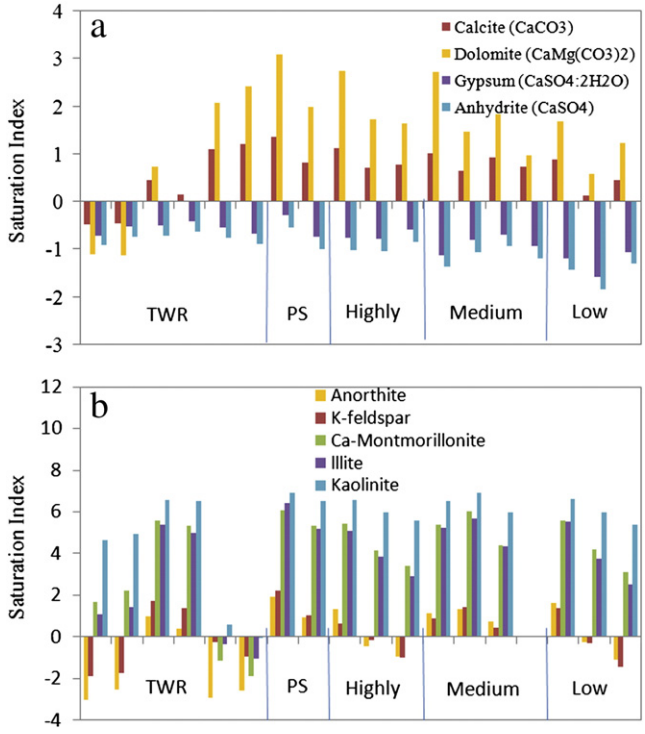

Fig. 7. Saturation indices showing carbonate precipitation and evaporate dissolution (a) and silicate weathering (b). PS indicates samples affected by point source pollution.

Conflict of interest

There are no known conflicts of interest associated with this publication and there has been no significant financial support for this work that could have influenced its outcome.

Acknowledgments

The study was supported by the Key Program of National Natural Science Foundation of China (No. 40830636), the State Basic Research Development Program (973 Program) of China (No. 2010CB428805) and the "Support program of AGSST for youth research" of Chiba University of Japan. The authors greatly thank reviewers for their good comments and suggestions on this manuscript. The authors greatly thank Dr. Jun Yang from University of Texas at Austin, USA for his kind help on the English revision of this paper.

References

Al-Charideh A, Hasan A. Use of isotopic tracers to characterize the interaction of water components and nitrate contamination in the arid Rasafeh area (Syria). Environ Earth Sci 2012:1–12.
Al-Kharabsheh A. Ground-water quality deterioration in arid areas: a case study of the Zerqa River basin as influenced by Khirbet Es-Samra waste water (Jordan). J Arid Environ 1999;43(3):227–39.
Appelo CAJ, Postma D. Geochemistry, groundwater and pollution. Netherlands: A.A. Balkema Publisher; 1994. p. 536.
Bai D, Ning Z. Analysis of reasons for the drying Lake Baiyangdian. China Flood Drought Manag 2007;2:46–8.
Belkhiri L, Boudoukha A, Mouni L, Baouz T. Application of multivariate statistical methods and inverse geochemical modeling for characterization of groundwater — a case study: Ain Azel plain (Algeria). Geoderma 2010;159(3–4):390–8.
Butler Il TW. Application of multiple geochemical indicators, including the stable isotopes of water, to differentiate water quality evolution in a region influenced by various agricultural practices and domestic wastewater treatment and disposal. Sci Total Environ 2007;388:149–67.
Cartwright I, Hall S, Tweed S, Leblanc M. Geochemical and isotopic constraints on the interaction between saline lakes and groundwater in southeast Australia. Hydrogeol J 2009;17(8):1991–2004.
Chisala BN, Lerner DN. Distribution of sewer exfiltration to urban groundwater. Water Manag 2008;161:333–41.
Clark I, Fritz P. Environmental isotopes in hydrogeology. Lewis, New York: CRC Press; 1997.
Craig H. Isotopic variations in meteoric waters. Science 1961;133(3465):1702–3.
Craig H, Gordon LI. Deuterium and oxygen 18 variations in the ocean and the marine atmosphere. In: Tongiorgi E, editor. Stable isotopes in oceanographic studies and paleotemperatures. Pisa: Laboratorio di Geologia Nucleare 1965. p. 9–130.
Cui B, Li X, Zhang K. Classification of hydrological conditions to assess water allocation schemes for Lake Baiyangdian in North China. J Hydrol 2010;385:247–56.
Freeze RA, Cherry JA. Groundwater. Englewood Cliffs. NJ: Prentice-Hall; 1979.
Geophysics Study Committee, Geophysics Research Forum NRC. Groundwater contamination. Washington, D.C.: National Academy Press; 1984
Gonfiantini R. Environmental isotopes in lake studies. In: Fritz P, Fontes J-Ch, editors. Handbook of environmental isotope geochemistry. The Terrestrial Environment. BAmsterdam, The Netherlands: Elsevier 1986. p. 113–68.
Guggenmos MR, Daughney CJ, Jackson BM, Morgenstern U. Regional-scale identification of groundwater–surface water interaction using hydrochemistry and multivariate statistical methods, Wairarapa Valley, New Zealand. Hydrol Earth Syst Sci 2011; 15(11):3383–98.
Horita J. Analytical aspects of stable isotopes in brines. Chem Geol Isot Geosci Section 1989;79:107–12.
Horita J, Wesolowski DJ. Liquid-vapor fractionation of oxygen and hydrogen isotopes of water from the freezing to the critical temperature. Geochim Cosmochim Acta 1994;58:3425–37.
Horita J, Rozanski K, Cohen S. Isotope effects in the evaporation of water: a status report of the Craig–Gordon model. Isot Environ Health Stud 2008;44(1):23–49.
Jankowski J, Acworth RI. Impact of debris-flow deposits on hydrogeochemical processes and the development of dryland salinity in the Yass River Catchment, New South Wales, Australia. Hydrogeol J 1997;5(4):71–88.
Kumar M, Ramanathan A, Keshari AK. Understanding the extent of interactions between groundwater and surface water through major ion chemistry and multivariate statistical techniques. Hydrol Process 2009;23(2):297–310.
Lerner D. Groundwater recharge. In: Saether O, de Caritat P, editors. Geochemical processes, weathering and groundwater recharge in catchments. Rotterdam: AA Balkema 1997. p. 109–50.
Liu C, Xie G, Huang H. Shrinking and drying up of Lake Baiyangdian wetland: a natural or human cause? Chin Geogr Sci 2006;16:314–9.
Lowe LD, Webb JA, Nathan RJ, Etchells T, Malano HM. Evaporation from water supply reservoirs: an assessment of uncertainty. J Hydrol 2009;376(1):261–74.
Majoube M. Fractionnement en oxygene-18 et en deuterium entre l'eau et sa vapeur. J Chem Phys 1971;197:1423–36.
McArthur JM, Sikdar PK, Hoque MA, Ghosal U. Waste-water impacts on groundwater: Cl/Br ratios and implications for arsenic pollution of groundwater in the Bengal Basin and Red River Basin, Vietnam. Sci Total Environ 2012;437(0):390–402.
Moiwo JP, Yang Y, Li H, Han S, Yang Y. Impact of water resource exploitation on the hydrology and water storage in Baiyangdian Lake. Hydrol Process 2010;24(21): 3026–39.
Otto M. Multivariate methods. In: Kellner R, Mermet JM, Otto M, Widmer HM, editors. Analytical chemistry. Weinheim: Wiley VCH 1998.
Panno S, Hackley K, Hwang H, Greenberg S, Krapac I, Landsberger S, et al. Characterization and identification of Na–Cl sources in ground water. Ground Water 2006;44(2): 176–87.
Parkhurst DL, Appelo CAJ. User's guide to PHREEQC — a computer program for speciation, reaction-path, 1D-transport, and inverse geochemical calculation. US Geological Survey; 1999 [Report No.: 99-4259].
Petelet-Giraud E, Négrel P, Gourcy L, Schmidt C, Schirmer M. Geochemical and isotopic constraints on groundwater–surface water interactions in a highly anthropized site. The Wolfen/Bitterfeld megasite (Mulde subcatchment, Germany). Environ Pollut 2007;148(3):707–17.
Qiu R, Li Y, Yang Z, Shi J. Influence of water quality change in Fu River on wetland Baiyangdian. Front Earth Sci China 2009;3(4):397–401.
Rieckermann J, Borsuk M, Reichert P, Gujer W. A novel tracer method for estimating sewer exfiltration. Water Resour Res 2005;41(5):1–11.
Scanlon BR, Healy RW, Cook PG. Choosing appropriate techniques for quantifying groundwater recharge. Hydrogeol J 2002;10:18–39.
Scanlon BR, Reedy RC, Tachovsky JA. Semiarid unsaturated zone chloride profiles: archives of past land use change impacts on water resources in the Southern High Plains, United States. Water Resour Res 2006;43:W06423.
Schirmer M, Leschik S, Musolff A. Current research in urban hydrogeology — a review. Advances in Water Resources 35th Year Anniversary Issue, 51(0). 2013. p. 280–91.
STATISTICA® 5.0 for Windows. Tulsa, OK: StatSoft, Inc.; 1998.
Wakida FT, Lerner DN. Non-agricultural sources of groundwater nitrate: a review and case study. Water Res 2005;39(1):3–16.
Wang S, Shao J, Song X, Zhang Y, Huo Z, Zhou X. Application of MODFLOW and geographic information system to groundwater flow simulation in North China Plain, China. Environ Geol 2008;55(7):1449–62.
Wang S, Tang C, Song X, Yuan R, Wang Q, Zhang Y. Using major ions and δ15N–NO_3^- to identify nitrate sources and fate in an alluvial aquifer. Environ Sci Process Impacts 2013;15:1430–43.
Ward Jr JH. Hierarchical grouping to optimize an objective function. J Am Stat Assoc 1963; 58:236–44.
Wu C. Landform environment and its formation in North China. Beijing: Science Press; 2008. p. 508.
Yuan R, Song X, Zhang Y, Han D, Wang S, Tang C. Using major ions and stable isotopes to characterize recharge regime of a fault-influenced aquifer in Beiyishui River watershed, North China Plain. J Hydrol 2011;405:512–21.
Zhang Z, Fei Y, Chen Z, Zhao Z, Xie Z, Wang Y, et al. Investigation and assessment of the sustainable use of groundwater in North China Plain. Beijing: Geological Publishing House; 2009 [Chinese].
Zhang B, Song X, Zhang Y, Han D, Tang C, Yu Y, et al. Hydrochemical characteristics and water quality assessment of surface water and groundwater in Songnen Plain, Northeast China. Water Res 2012;46(8):2737–48.